On the Origin of α- and β-Agostic Distortions in Early-Transition-Metal Alkyl Complexes

Dimitrios A. Pantazis,[†] John E. McGrady,*[,†] Maria Besora,[‡] Feliu Maseras,[‡,§] and Michel Etienne[△]

WestCHEM, Department of Chemistry, Joseph Black Building, University of Glasgow, Glasgow G12 8QQ, United Kingdom, Unitat de Química Física, Edifici Cn, Universitat Autònoma de Barcelona, 08193 Bellaterra, Catalonia, Spain, Institute of Chemical Research of Catalonia (ICIQ), Avgda. Països Catalans 16, 43007 Tarragona, Spain, and Laboratoire de Chimie de Coordination du CNRS, UPR 8241, liée par conventions à l'Université Paul Sabatier et à l'Institut National Polytechnique de Toulouse, 205 Route de Narbonne, 31077 Toulouse, Cedex 4, France

Received December 3, 2007

Density functional theory is used to explore the origins of the α- and β-C−H agostic distortions in two isomers of $Tp^{Me2}NbCl(MeC{\equiv}CPh)(i\text{-}Pr)$, both of which have been characterized experimentally. We first establish that our computational methodology provides a solid foundation on which to build such a model by showing that it reproduces a wide range of experimental observables, including structural, thermodynamic, and kinetic data and spin–spin coupling constants, $^1J_{C-H}$, of the isopropyl ligand. Analysis of the converged electron density for the β-agostic rotamer reveals that the molecular graph is highly dependent on functional: in some cases, bond and ring critical points can be located, while in others, they merge into a singularity, despite the fact that the associated changes in geometry are almost imperceptible. The unpredictable behavior of the molecular graph confirms that the electron density in the region between the metal and the C−H bond is almost homogeneous, but an accurate description of this region is clearly critical because only those functionals that conform to the uniform electron gas (UEG) limit are able to locate the β-agostic minimum. Taken together, these observations suggest that through-space interactions between the C−H bond and the metal make an important contribution to the stability of the system. In contrast, the molecular graph for the α-agostic isomer is completely independent of functionals: no Nb···H critical point has ever been located. This, combined with the fact that the α-agostic structures optimized with UEG and non-UEG functionals are very similar, suggests that through-space interactions between the C−H σ bond and the metal are less important in this case. Analysis of the Kohn–Sham and natural bond orbitals for the α-agostic isomer suggests that the distortion is instead driven by delocalization of the Nb−C_α σ bonding electrons onto the unsaturated alkyne ligand. The underlying cause is the energy mismatch between the early-transition-metal d orbitals and the lone pair on the formally anionic alkyl ligand, which forces delocalization of the Nb−C_α bonding electrons onto the π* orbitals of the alkyne ligand. The same mechanism is also important in the β-agostic system, although in this case, the agostic distortion is further stabilized by a through-space interaction between the β-C−H σ bond and the metal.

Introduction

Ever since the term "agostic bonding" was coined by Green in 1983,[1,2] the precise nature of the interaction between the C−H group and the metal atom has been the center of debate. Perhaps the simplest description of the bonding involves donation of the electrons in the C−H σ bond to the metal center,[3] and a 3-center−2-electron model[4] remains the textbook explanation. The structural similarities between agostic complexes and η^2-coordinated diatomic ligands such as H_2 have also encouraged speculation that back-donation into the C−H σ* orbital may play a role,[5,6] although the abundance of main-group and early-transition-metal agostics suggests this cannot be the dominant mechanism in all cases. Within the general class of agostic complexes, there is an important distinction to be made between α- and β-C−H agostic structures: the earliest studies using extended Hückel theory suggested that while the 3-center−2-electron model was appropriate for the β-C−H agostic bonds,[7] there was no evidence for significant sharing of electron density between the hydrogen and the metal in the α-agostic analogues.

* Corresponding author.
[†] University of Glasgow.
[‡] Universitat Autònoma de Barcelona.
[§] ICIQ.
[△] LCC Toulouse.

(1) Brookhart, M.; Green, M. L. H. *J. Organomet. Chem.* **1983**, *250*, 395.
(2) Brookhart, M.; Green, M. L. H.; Wong, L.-L. *Prog. Inorg. Chem.* **1988**, *36*, 1.
(3) (a) Trofimenko, S. *J. Am. Chem. Soc.* **1968**, *90*, 4754. (b) Trofimenko, S. *Inorg. Chem.* **1970**, *9*, 2493.
(4) Cotton, F. A.; LaCour, T.; Stanislowski, A. G. *J. Am. Chem. Soc.* **1974**, *96*, 754.
(5) (a) Butts, M. D.; Bryan, J. C.; Luo, X.-L.; Kubas, G. *Inorg. Chem.* **1997**, *36*, 3341. (b) Nikonov, G. I.; Mountford, P.; Ignatov, S. K.; Green, J. C.; Leech, M. A.; Kuzmina, G. L.; Razuvaev, A. G.; Rees, N. H.; Blake, A. J.; Howard, J. A. K.; Lemenovskii, D. A. *J. Chem. Soc., Dalton Trans.* **2001**, 2903.
(6) (a) Ziegler, T.; Tschinke, V.; Becke, A. *J. Am. Chem. Soc.* **1987**, *109*, 1351. (b) Han, Y.; Deng, L.; Ziegler, T. *J. Am. Chem. Soc.* **1997**, *119*, 5939.
(7) Demolliens, A.; Jean, Y.; Eisenstein, O. *Organometallics* **1986**, *5*, 1457.

10.1021/om701211r CCC: $40.75
Publication on Web 02/19/2008

The short M···H separation in the latter was instead proposed to result from a canting of the alkyl group in order to optimize the strength of the M−C bond,[8,9] and similar distortions have subsequently been noted for acyl complexes.[10]

The development of quantitative theoretical tools over the past decade has encouraged several groups to reassess the nature of the agostic bond. Popelier has pioneered the use of the quantum theory of atoms in molecules (QTAIM)[11] approach in this context and argued that the presence of a bond critical point (BCP) between the metal and the β hydrogen in $[(C_2H_5)TiCl_2]^+$ was indicative of a β-C−H agostic bond.[12] In contrast, other groups have shown that no such critical point is present in α-C−H agostic bonds,[13] suggesting that they have a fundamentally different origin. Indeed, Dobado and co-workers have argued that the term α-agostic "bond" should be avoided and replaced with "α-agostic geometry".[14] Recent work by Scherer, McGrady and co-workers on d^0 transition-metal alkyls has further shown that, even for β-C−H agostic interactions, the appearance of a BCP between metal and hydrogen is highly dependent on the chosen computational methodology.[15] Moreover, they have argued that the bending of the alkyl group (and, hence, the close proximity of the metal and hydrogen) in these cases is caused not by direct M−H interaction but rather by negative hyperconjugation of the electrons in the M−C σ bond.[16] Within this framework, the bonding between the metal center and the entire alkyl unit is controlled by a single doubly occupied bonding orbital. Thus, it seems that early-transition-metal agostic bonds are fundamentally different from their late-transition-metal analogues and, moreover, that α-agostic bonds are fundamentally different from their β-agostic counterparts. This somewhat confusing situation was summarized neatly by Clot and Eisenstein in their recent review entitled "Agostic Interactions from a Computational Perspective: One Name, Many Interpretations".[17]

In view of the ongoing debate regarding the precise nature of the bonding, a more pragmatic definition is often adopted, based on the structural consequences of agostic interactions rather than their underlying cause. In this spirit, Scherer et al. proposed the working definition that *agostic interactions are characterized by the distortion of an organometallic moiety which brings an appended C−H bond into close proximity with the metal center*.[15] The structural distortions in question typically involve bending of the alkyl chain and are, therefore, relatively undemanding in energetic terms. The importance of this point

Scheme 1. X-ray structure of the β-agostic isomer of $Tp^{Me2}NbCl(MeC{\equiv}CPh)(i\text{-}Pr)$ and schematic representation of three rotamers generated by rotation about the Nb−C_α bond. The X-ray structure corresponds to rotamer 3[20]

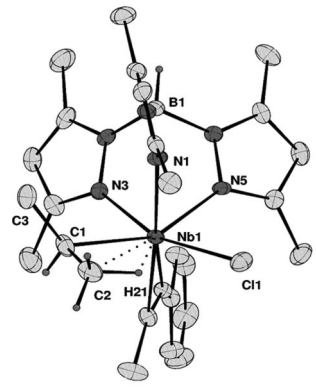

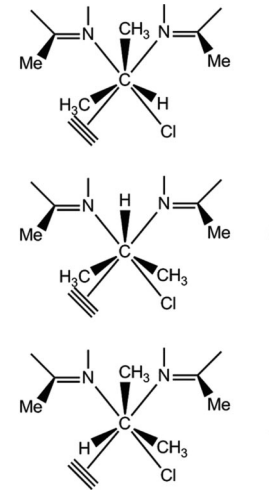

in the context of computational studies cannot be overemphasized because the ability to reproduce the key features of the experimental geometry is typically the first criterion used to establish the validity of any given model chemistry. This is clearly a rather poor criterion if we restrict attention to the carbon framework because almost any type of interaction (steric, covalent, electrostatic), whether it be real or an artifact of the modeling process, may be strong enough to induce this bending. Thus, the successful optimization of an agostic structure according to the definition set out above is no guarantee that the theoretical model has captured the true essence of the agostic "bond" or "interaction". We illustrated this point graphically in a recent paper,[18] where we showed that, although our previous work[19–21] using a hybrid B3LYP/MM protocol reproduced the characteristic distortions of the alkyl backbone in the β-agostic isomer of $Tp^{Me2}NbCl(MeC{\equiv}CPh)(i\text{-}Pr)$ (shown in Scheme 1), the apparently impressive agreement with experiment was, in fact, the result of compensation of two errors. One the one hand, the B3LYP functional[22–24] (along with others that do not conform to the UEG limit) underestimates the strength of the β-C−H agostic interaction[25] relative to the competing Nb−Cl π bonding, while on the other hand, our chosen quantum mechanical/molecular mechanics (QM/MM) partition introduced a spurious positive charge into the QM region. The additional electrostatic component to the Nb···C−H interaction compensates for the intrinsic underestimation of the agostic bond strength, and the net result is an apparently excellent structure but for the wrong reasons: the model was not capturing the essence of the agostic interaction. Clear signs of the error compensation can be detected in the remainder of the niobium coordination sphere, particularly the Nb−Cl bond, which is some 0.07 Å shorter than experiment, reflecting the unbalanced

(8) Eisenstein, O.; Jean, Y. *J. Am. Chem. Soc.* **1985**, *107*, 1177.
(9) Goddard, R. J.; Hoffmann, R.; Jemmis, E. D. *J. Am. Chem. Soc.* **1980**, *102*, 7667.
(10) Ujaque, G.; Maseras, F.; Lledos, A.; Contreras, L.; Pizzano, A.; Rodewald, D.; Sanchez, L.; Carmona, E.; Monge, A.; Ruiz, C. *Organometallics* **1999**, *18*, 3294.
(11) (a) Bader, R. F. W. *Atoms in Molecules: A Quantum Theory*; Oxford University Press: Oxford, U.K., 1990. (b) Popelier, P. *Atoms in Molecules, An Introduction*; Pearson Education: Harlow, 2000. (c) Bader, R. F. W. *Chem. Rev.* **1991**, *91*, 893.
(12) Popelier, P. L. A.; Logothetis, G. *J. Organomet. Chem.* **1998**, *555*, 101.
(13) Thakur, T. S.; Desiraju, G. R. *THEOCHEM* **2007**, *810*, 143.
(14) Vidal, I.; Melchor, S.; Alkorta, I.; Elguero, J.; Sundberg, M. R.; Dobado, J. A. *Organometallics* **2006**, *25*, 5638.
(15) (a) Scherer, W.; McGrady, G. S. *Angew. Chem., Int. Ed.* **2004**, *43*, 1782. (b) Scherer, W.; Sirsch, P.; Shorokhov, D.; Tafipolsky, M.; McGrady, G. S.; Gullo, E. *Chem.−Eur. J.* **2003**, *9*, 6057.
(16) (a) Haaland, A.; Scherer, W.; Ruud, K.; McGrady, G. S.; Downs, A. J.; Swang, O. *J. Am. Chem. Soc.* **1998**, *120*, 3762. (b) Scherer, W.; Hieringer, W.; Spiegler, M.; Sirsch, P.; McGrady, G. S.; Downs, A. J.; Haaland, A.; Pedersen, B. *Chem. Commun.* **1998**, 2471. (c) Scherer, W.; Sirsch, P.; Grosche, M.; Spiegler, M.; Mason, M.; Gardiner, M. G. *Chem. Commun.* **2001**, 2072.
(17) Clot, E.; Eisenstein, O. *Struct. Bonding (Berlin)* **2004**, *113*, 1.
(18) Pantazis, D. A.; McGrady, J. E.; Maseras, F.; Etienne, M. *J. Chem. Theory Comput.* **2007**, *3*, 1329.
(19) Jaffart, J.; Mathieu, R.; Etienne, M.; McGrady, J. E.; Eisenstein, O.; Maseras, F. *J. Chem. Soc., Chem. Commun.* **1998**, 2011.
(20) Jaffart, J.; Etienne, M.; Maseras, F.; McGrady, J. E.; Eisenstein, O. *J. Am. Chem. Soc.* **2001**, *123*, 6000.
(21) Besora, M.; Maseras, F.; McGrady, J. E.; Oulié, P.; Dinh, D. H.; Duhayon, C.; Etienne, M. *Dalton Trans.* **2006**, 2362.
(22) Becke, A. D. *J. Chem. Phys.* **1993**, *98*, 5648.
(23) Stevens, P. J.; Devlin, J. F.; Chabalowski, C. F.; Frisch, M. J. *J. Phys. Chem.* **1994**, *98*, 11623.
(24) Lee, C.; Yang, W.; Parr, R. G. *Phys. Rev. B* **1988**, *37*, 785.
(25) Ruiz, E.; Salahub, D. R.; Vela, A. *J. Phys. Chem.* **1996**, *100*, 12265.

description of Nb−Cl π and C−H agostic bonding. Our subsequent reevaluation using a full QM protocol with functionals that do obey the UEG limit (PBE0, for example) afforded a much improved description of the competition between C−H agostic and Nb−Cl π bonding, and hence a significantly longer Nb−Cl bond length. As a result of this recent theoretical work, we now believe that we have a computational method that truly captures the essential features of the β-C−H agostic interaction rather than simply reproducing the distortion of the carbon backbone.

The Tp^{Me2}NbCl(MeC≡CPh)(*i*-Pr) system is one of the very few examples where both α- and β-agostic structures have been characterized (rotamers **1** and **3** in Scheme 1), and it therefore offers a unique opportunity to benchmark our theoretical model against a broader range of experimental data. In the first section of this paper, we show that the PBE0 functional is able to reproduce not just the structure of the β-agostic isomer but also the relative energies of the α- and β-agostic isomers, the barrier separating them, and the spin–spin coupling constants, $^1J_{C-H}$, observed in their NMR spectra. On the basis of this close agreement between experiment and theory, we believe that the computed electronic structure provides a solid foundation for exploring the underlying cause of the agostic distortion. The second section of the paper then describes an analysis of the Kohn–Sham and natural bond orbitals (NBOs) of the α- and β-agostic isomers, along with their computed electron densities, the aim being to develop a deeper understanding of these apparently quite different interactions.

Results and Discussion

Potential Energy Surface for Rotation about the Nb−C Bond in Tp^{Me2}NbCl(MeC≡CMe)(*i*-Pr). As we have noted in previous papers, the existence of a dynamic equilibrium between α- and β-agostic structures in the Tp^{Me2}NbCl(R′C≡CR″)(R) family of complexes stems principally from the unique topological profile of the hydrotris(3,5-dimethylpyrazolyl)borate (Tp^{Me2}) ligand: the alkyl substituent R is located in a tight steric pocket defined by the pendant methyl groups on two *cis*-pyrazolyl rings, whose steric bulk restricts rotation about the Nb−C_α bond.[19–21,26] For the *i*-Pr complex, Tp^{Me2}NbCl(MeC≡CPh)(*i*-Pr), this means that distinct α- and β-agostic isomers (**1** and **3**, respectively, in Scheme 1) can be observed by NMR spectroscopy, with the latter being the more stable ($\Delta G°_{193} = -2.2 \pm 0.1$ kJ mol^{-1}; $\Delta H° = -7.4 \pm 0.1$ kJ mol^{-1}).[19,20] Moreover, the activation parameters for the interconversion of the two isomers have been estimated at $\Delta G_{193}^{\ddagger} = 47.5 \pm 2.5$ kJ mol^{-1} and $\Delta H^{\ddagger} = 58.8 \pm 2.5$ kJ mol^{-1}, values that are substantially higher than the intrinsic strength of the agostic interaction,[15,17,27] confirming the key role of the steric environment in stabilizing the two distinct rotamers. In contrast, there was no evidence for the third rotamer, **2**, where the α hydrogen lies in the least sterically crowded position between the two nitrogens. This wealth of thermodynamic and kinetic data prompted us to explore the complete potential energy surface defined by a 360° rotation about the Nb−C_α bond, encompassing the three structures shown in Scheme 1 as well as the transition states that link them.

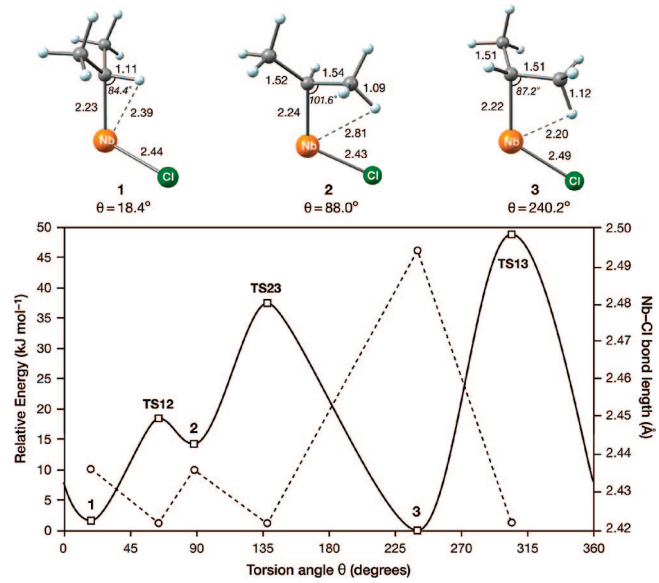

Figure 1. Top: selected optimized parameters of the isopropyl minima. Bottom: schematic diagram of the potential energy (left axis, solid line) for rotation about the Nb−C_α bond and concomitant changes in the Nb−Cl bond length (right axis, dotted line).

The computed potential energy surface for rotation about the Nb−C_α bond in Tp^{Me2}NbCl(MeC≡CMe)(*i*-Pr) [calculations were performed on the but-2-yne complex rather than its phenylpropyne analogue for computational expedience; test calculations have shown that differences between the optimized structures of the two are negligible[18]] is shown in Figure 1, where the torsion angle θ is defined as the Cl−Nb−C_α−H dihedral ($0° \le \theta \le 360°$). Optimized bond lengths and angles for the three minima are collected in Table 1, where B3LYP-optimized parameters are also shown for comparison. Consistent with experiment, the global minimum is the β-agostic structure **3**, the computed geometry of which was discussed in detail in our recent benchmark study.[18] We simply reiterate here that all of the key features of the optimized structure are in excellent agreement with the X-ray data, provided that the chosen functional adheres to the UEG limit (PBE0, for example). The most noteworthy features are the acute Nb−C_α−C_β angle of 87.2°, the elongated C_β−H bond length (1.12 vs 1.09 Å for nonagostic C−H bonds), the obtuse Cl−Nb−C_α angle (121.9°), and the rather long Nb−Cl bond (2.49 Å). Non-UEG functionals such as B3LYP, in contrast, fail to locate a β-agostic minimum of any kind. Rotamer **1** lies only 1.5 kJ mol^{-1} above the global β-agostic minimum (cf. $\Delta H° = 7.4 \pm 0.1$ kJ mol^{-1}), and its structure bears the classic hallmarks of an α-agostic complex: an acute Nb−C_α−H angle of 84.4° and an elongated C_α−H bond (1.11 vs 1.09 Å in **3**). [Optimized Cartesian coordinates and selected bond lengths for all stationary points shown in Figure 1 are given in the Supporting Information.] The Nb−Cl bond length in **1** (2.44 Å) is also much shorter than that in **3**, and the Cl−Nb−C_α angle is significantly less obtuse (106.0° compared to 120.4°). We have previously highlighted the Nb−Cl bond length as an indirect but sensitive probe of β-agostic bonding, where the C−H σ bond competes with the π lone pairs on the chloride ligand for vacant d orbital space on the niobium center. The short Nb−Cl bond in **1** therefore offers a clear indication that, whatever the origin of the α-agostic interaction, it does *not* compete with Cl π orbitals for the vacant metal-based orbital in the same way as its β-agostic counterpart. The fundamental difference between α- and β-C−H agostic bonds in the two rotamers is further highlighted by the sensitivity

(26) (a) Teuma, E.; Etienne, M.; Donnadieu, B.; McGrady, G. S. *New J. Chem.* **2006**, *30*, 409. (b) Jaffart, J.; Cole, M. L.; Etienne, M.; Reinhold, M.; McGrady, J. E.; Maseras, F. *Dalton Trans.* **2003**, 4057. (c) Jaffart, J.; Etienne, M.; Reinhold, M.; McGrady, J. E.; Maseras, F. *Chem. Commun.* **2003**, 876.

(27) Von Frantzius, G.; Streubel, R.; Brandhorst, K.; Grunenberg, J. *Organometallics* **2006**, *25*, 118.

Table 1. Selected Optimized Bond Lengths (Å) and Angles (deg) for 1−3

rotamer	functional	Nb–Cl	Nb–C_α	Nb−C_α−H_α	Nb–H_α	C_α–H	Nb−C_α−C_β	Nb–C_β	Nb–H_β	C_β–H
1	PBE0	2.44	2.23	84.4	2.39	1.11				
	B3LYP	2.46	2.26	86.0	2.45	1.11				
2	PBE0	2.43	2.24				101.6	2.96	2.81	1.09
	B3LYP	2.44	2.28				106.7	3.10	3.04	1.09
3[18]	PBE0	2.49	2.22				87.2	2.62	2.20	1.12
	B3LYP	2.44	2.28				109.3	3.15	3.23	1.09

of the optimized geometries to the chosen density functional: while the β-agostic structure of **3** is only reproduced accurately by functionals such as PBE0 that adhere to the UEG limit,[18] the bond lengths and angles of the α-agostic analogue, **1**, are very similar for the PBE0 and B3LYP (non-UEG) functionals (Table 1). The fact that the accurate description of near-homogeneous electron density distributions provided by UEG functionals is apparently critical for the β-agostic structure but not for its α-agostic counterpart provides compelling evidence that direct through-space Nb···C−H interactions are important in the former but not in the latter.

Of the three transition states that connect the minima **1**−**3**, the highest in energy is TS13, where the two methyl groups on the alkyl chain lie directly under two pendant methyls of the Tp^{Me2} ligand, as a result of which one Nb–N bond is elongated by approximately 0.1 Å (see the Supporting Information). The two remaining transition states, TS23 and TS12 (37.4 and 18.4 kJ mol^{-1}, respectively), are less sterically hindered, although some elongation of the Nb−N bonds occurs in both cases. Thus, the barrier reflects not just the intrinsic strength of the agostic bond but also a significant steric component associated with the disruption of the niobium coordination sphere. The computed profile also suggests that the dynamic interconversion of **1** and **3** will *not* occur directly through a 120° rotation via TS13 but rather through a 240° rotation via both TS23 and TS12, as well as the metastable intermediate, **2**. The maximum barrier along the **1** → TS12 → **2** → TS23 → **3** pathway is 37.4 kJ mol^{-1}, in reasonable agreement with an experimental $\Delta G_{193}^{\ddagger}$ of 47.5 ± 2.5 kJ mol^{-1} for Tp^{Me2}NbCl(MeC≡CPh)(*i*-Pr).

Spin–Spin Coupling Constants, $^1J_{C-H}$. In the previous sections, we have emphasized the structural criteria that lead to the identification of a given complex as agostic or otherwise. The use of structural data is, however, somewhat limited by the fact that changes in C−H bond lengths are typically on the order of a few hundredths of an angstrom, often below the resolution of diffraction experiments. This limitation is particularly pressing in α-agostic structures, where diagnostic distortions of the alkyl backbone are absent. In such circumstances, C−H coupling constants, $^1J_{C-H}$, are commonly used to identify agostic species in solution: $^1J_{C-H}$ values in the region of 100 Hz[20,28] clearly distinguish agostic C−H bonds from their nonagostic counterparts, where coupling constants are typically on the order of 120−130 Hz.[29] The computation of spin–spin coupling constants has recently been reviewed by Autschbach,[30] while Eisenstein[31] and Clot[32] have applied this methodology to agostic complexes. The C−H bonds of the completely nonagostic methyl groups in rotamer **1** (α-agostic) provide a convenient internal reference point for the following discussion: the average of the computed values, 115 Hz, is approximately 8 Hz lower than the experimental value of 123 Hz. The computed $^1J_{C-H}$ for the α hydrogen is significantly lower at 95 Hz and is in excellent agreement with experiment ($^1J_{C-H}$ = 100 ± 5 Hz).[20] In the absence of crystallographic data for the α-agostic rotamer, the convergence of computed and experimental coupling constants provides the most convincing evidence that our theoretical model captures the essential features of the α- as well as β-agostic interactions. For the β-agostic C−H bond in **3**, the comparison with experiment is complicated by the fact that the rotation of the agostic methyl cannot be frozen out even at very low temperatures, as a result of which only an average $^1J_{C-H}$ is observed, coincidentally at exactly the same frequency (123 Hz) as the C−H bonds of the nonagostic methyl group. The calculations establish that the β-agostic C−H bond does have a dramatically reduced $^1J_{C-H}$ of 90 Hz, but this is offset by a concomitant increase for the two nonagostic C−H bonds (124 and 125 Hz) caused by rehybridization of the β carbon. The average of these three computed values (90, 124, and 125 Hz) is 113 Hz, very similar to computed values for the reference nonagostic methyl groups (115 Hz). Rotational averaging is the norm in β-agostic systems, and in such circumstances, $^1J_{C-H}$ for the nonagostic α-C−H bond is typically used as a diagnostic tool because the rehybridization at the α carbon also results in an increased coupling constant (expt: $^1J_{C-H}$ = 138 Hz in this case). The computed value of 128 Hz is again somewhat lower than the experiment, but it is 13 Hz higher than values for the reference sp^3-hybridized methyl C−H bonds and fully 33 Hz higher than the α-agostic C−H bond in rotamer **1**. Overall, although the values of $^1J_{C-H}$ are underestimated by approximately 8–10 Hz in each case, the key experimental trends are reproduced with remarkable accuracy.

Analysis of the Electron Structure: Origin of the α- and β-C−H Agostic Bonds in Tp^{Me2}NbCl(MeC≡CMe)(*i*-Pr). In the previous sections, we have shown that the computed properties of both α- and β-C−H agostic isomers are fully consistent with all of the available structural, thermodynamic, kinetic, and spectroscopic data. This gives us confidence that our chosen theoretical method is capturing the essential physics that lies behind these interactions and therefore that the converged electron density should provide a firm foundation for the construction of a bonding model. In the following section, we use the QTAIM approach,[11] along with an analysis of the Kohn–Sham and NBOs, to explore the origins of the β- and α-agostic distortions in **3** and **1**.

We noted in the Introduction that our choice of the PBE0 functional for this work was guided by our earlier finding that the UEG limit is critical for modeling the β-agostic geometry of rotamer **3** (see Table 1).[18] However, despite the patently "agostic" optimized structure of **3** shown in Figure 1, we have been unable to locate a BCP between the agostic hydrogen and the niobium center using this PBE0 functional. In contrast, the

(28) (a) Pilyugina, T. S.; Schrock, R. R.; Hock, A. S.; Muller, P. *Organometallics* **2005**, *24*, 1929. (b) Singha, A.; Schrock, R. R. *Organometallics* **2004**, *23*, 1643.

(29) Crabtree, R. H. *The Organometallic Chemistry of the Transition Metals*; Wiley: New York, 2001.

(30) Autschbach, J. *Struct. Bonding (Berlin)* **2004**, *112*, 1.

(31) (a) Solans-Montfort, X.; Eisenstein, O. *Polyhedron* **2006**, *25*, 339. (b) Solans-Montfort, X.; Clot, E.; Copéret, C.; Eisenstein, O. *Organometallics* **2005**, *24*, 1586.

(32) (a) Bolton, P. D.; Clot, E.; Cowley, A. R.; Mountford, P. *Chem. Commun.* **2005**, 3313. (b) Bolton, P. D.; Clot, E.; Adams, N.; Dubberley, S. R.; Cowley, A. R.; Mountford, P. *Organometallics* **2006**, *25*, 2806.

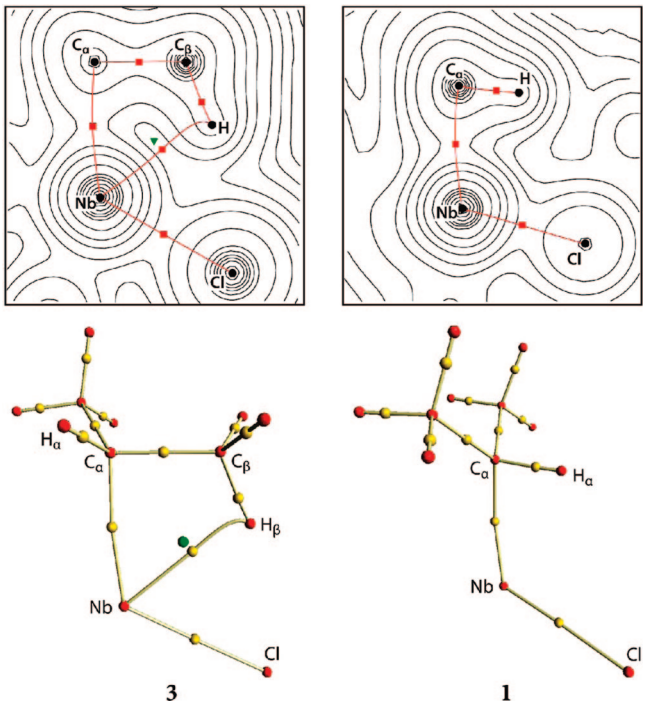

Figure 2. Density maps (TPSS functional) drawn on the agostic planes (top) and partial molecular graphs (bottom) of isopropyl rotamers **3** and **1**. Red spheres indicate nuclear attractors, and yellow and green spheres correspond to (3, −1) bond and (3, +1) ring critical points, respectively.

molecular graph obtained using the TPSS functional,[33] shown in Figure 2, features a bond path connecting the metal to the agostic hydrogen, with a characteristic inward curvature in the vicinity of the C−H bond. The molecular graph, in fact, closely resembles the archetypal example of β-agostic bonding reported by Popelier and Logothetis in their study of agostic titanium chloroalkyl systems.[12] The Nb···H BCP is, however, very close to the ring critical point, and it is therefore unsurprising that very small changes in geometry or indeed methodology can cause them to merge into a singularity. It is important to emphasize that although the TPSS functional resolves the ring and Nb···H critical points while the PBE0 functional does not, the optimized structures and electron density profiles in the agostic region are almost identical for the two functionals.[18] The apparently erratic behavior of the molecular graph is intimately connected to the dependence of the structure on functional: the very fact that the UEG limit is critical for the modeling of the β-agostic structure immediately tells us that electron density in the important region between the Nb and H atoms is highly homogeneous, and it is precisely these situations where characterization of the curvature of ρ is most difficult.

The location of a Nb···H BCP for the TPSS functional suggests that a direct interaction between the metal and the C−H bond cannot be discounted in the case of β-agostic structures, although there appears to be no strong link between the molecular graph and the optimized structure. In marked contrast, a Nb···H bond path is *never* found for the α-C−H agostic structure, **1**, regardless of the functional (the results using TPSS are shown in Figure 2, but the molecular graph is identical with that of PBE0 or indeed a non-UEG functional such as B3LYP). The lack of BCPs in this case is fully consistent with other studies of α-agostic complexes, where bond paths between metal and hydrogen are conspicuously absent.[14] The topology of the electron density does, therefore, seem to eliminate the possibility of a direct interaction between the metal center and the C−H bond in the case of the α-C−H agostic isomer.

The Kohn–Sham orbitals of the α- and β-agostic structures shown in Figure 3 offer a complementary perspective on the origin of the agostic interactions. In the α-agostic structure, **1**, direct overlap between the C−H σ and metal-based orbitals is clearly negligible, so what causes the alkyl group to distort? In their study of β-agostic structures in d^0 transition-metal complexes, Scherer et al. have argued that the key stabilizing influence is the delocalization of the M−C σ bonding electrons over the framework of the alkyl ligand: in effect negative hyperconjugation.[15] Stabilization of the M−C bonding electrons also lies at the heart of Eisenstein's early explanation of α-agostic bonding,[8] although in this case, delocalization was into metal-based orbitals. In **1**, the highest occupied molecualr orbital (HOMO) clearly has dominant Nb−C σ bonding character, but it is also significantly delocalized onto the π^* orbital on the alkyne unit. The overlap of the alkyl- and alkyne-based orbitals is enhanced by a canting of the Nb−C_α σ orbital (shown as a dashed line in Figure 3), which, in turn, forces one of the substituents on the α carbon toward the metal. In this context, it is interesting to note that exchange of the CH_2R and Me groups has been observed in Tp^{Me2}NbCl(PhC≡CMe)(CH_2R), indicating that reversible migration of an alkyl group from the metal to the alkyne ligand is a relatively facile process.[20] The α-agostic equilibrium structure of **1** can be viewed as an early stage of the reaction coordinate for this exchange process. We noted above that the presence of a Nb···H bond path in **3** (at least with some functionals) suggests that, unlike the α-agostic case, direct overlap between the β C−H σ bonding orbital and a vacant metal-based orbital does play a role in stabilizing the system. This overlap is apparent in the lowest unoccupied molecular orbital of **3** shown in Figure 3, where there is substantial mixing of C−H σ and metal d character. However, the delocalization of the Nb−C σ bonding electrons into the π^* orbital of the alkyne identified for the α-agostic isomer is again apparent in the HOMO, suggesting that both mechanisms contribute to the stability of the β-agostic rotamer.

The model of agostic bonding that emerges from the Kohn–Sham orbitals is reinforced by a NBO[34] analysis of the α- and β-agostic isomers. The NBO analysis is based on the definition of a Lewis reference structure, from which delocalization corrections are calculated as donor–acceptor interactions between occupied and unoccupied orbitals, φ_i and φ_j, using second-order perturbation theory: $\Delta E(i/j) = -n_i(\langle\varphi_i|\hat{F}|\varphi_j\rangle^2)/\epsilon_j - \epsilon_i$, where $\hat{F}$ is the Kohn–Sham operator, n_i is the occupation of the donor orbital, and ϵ_i and ϵ_j are the energies of the donor and acceptor orbitals, respectively. In the β-agostic rotamer **3**, there is a significant second-order energy correction between the occupied β-C−H bonding orbital (NBO 1 in Figure 4) and a vacant d orbital on niobium (NBO 4; $\Delta E(1/4) = 130$ kJ mol^{-1}), supporting the classical 3-center−2-electron bond model. There is, however, also a substantial contribution ($\Delta E(3/5) + \Delta E(3/6) = 83$ kJ mol^{-1}) from the interaction between the Nb−C_α bonding orbital (NBO 3) and the two localized Nb−C(alkyne) σ^* orbitals (NBOs 5 and 6) supporting our proposal that delocalization of the Nb−C bonding electrons onto the coordinated alkyne also plays an important role. For the

(33) Tao, J.; Perdew, J. P.; Staroverov, V. N.; Scuseria, G. E. *Phys. Rev. Lett.* **2003**, *91*, 146401.

(34) Reed, A. E.; Curtiss, L. A.; Weinhold, F. *Chem. Rev.* **1988**, *88*, 899.

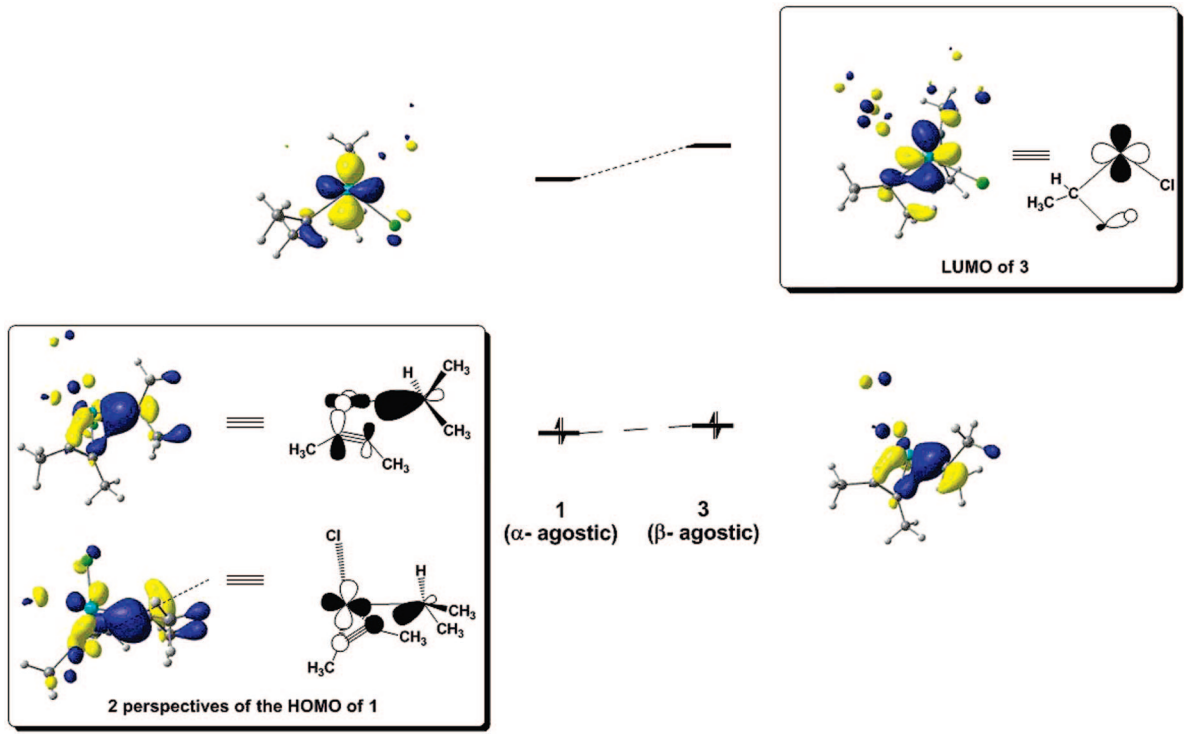

Figure 3. Frontier Kohn–Sham orbitals of α- and β-C−H agostic structures of $Tp^{Me2}NbCl(MeC{\equiv}CMe)(i\text{-}Pr)$. The HOMO of **1** is shown from two distinct orientations. Contour value: 0.0622 (e $Å^{-3})^{1/2}$. The dashed line illustrates the tilting of the Nb−C bonding orbital relative to the Nb−C axis.

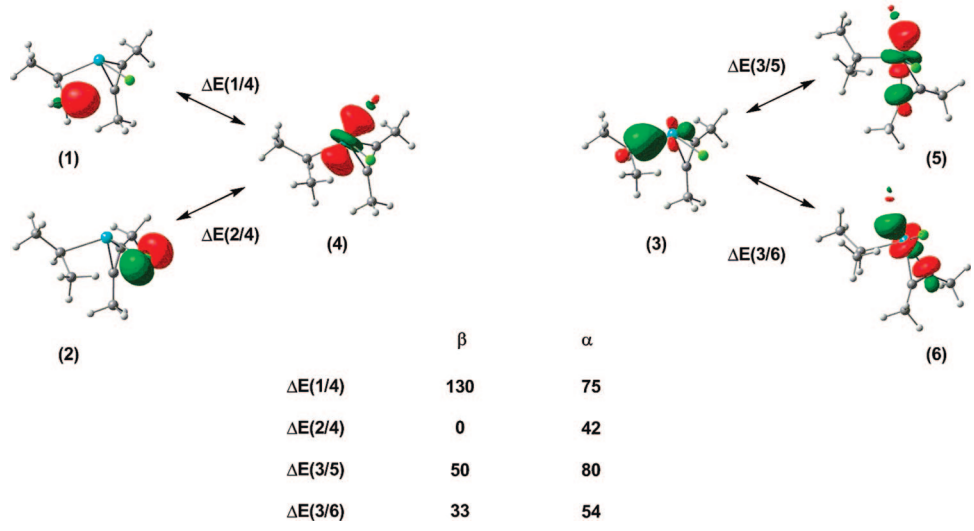

	β	α
ΔE(1/4)	130	75
ΔE(2/4)	0	42
ΔE(3/5)	50	80
ΔE(3/6)	33	54

Figure 4. NBOs of the β-C−H agostic structure of $Tp^{Me2}NbCl(MeC{\equiv}CMe)(i\text{-}Pr)$. Orbitals for the α-agostic isomer are almost identical with the exception of (1), where the C−H bonding orbital is naturally localized on the α-C−H unit. Contour value: 0.0899 (e $Å^{-3})^{1/2}$. Second-order interaction energies, ΔE, in kJ mol^{-1}.

α-agostic rotamer, **1**, the interaction between the C−H bonding orbital and the metal d is substantially reduced ($\Delta E(1/4) = 75$ kJ mol^{-1}) and is replaced by donation from a chloride lone pair (NBO 2) into the same orbital ($\Delta E(2/4) = 42$ kJ mol^{-1}), again reflecting the competition between C−H bonding electrons and chloride lone pairs for vacant orbital space on the metal. In addition to this redistribution within the alkyl−Nb−Cl unit, there is also an increase in the strength of the interaction between the Nb−C_α bonding orbital (NBO 3) and the two localized Nb−C(alkyne) σ^* orbitals (NBOs 5 and 6) ($\Delta E(3/5) + \Delta E(3/6) = 134$ kJ mol^{-1}). The classical 3-center−2-electron agostic interaction in **3** is therefore replaced by a stronger Cl−Nb π bond *and* enhanced delocalization of the Nb−C_α σ bond into vacant orbitals on the alkyne unit in **1**.

Summary

In the initial section of this manuscript, we have shown that functionals such as PBE0 that conform to the UEG limit provide excellent agreement with all available structural, thermodynamic, and kinetic data for the α/β-C−H agostic equilibrium in $Tp^{Me2}NbCl(MeC{\equiv}CPh)(i\text{-}Pr)$. Moreover, although the computed spin–spin coupling constants, $^1J_{C-H}$, are uniformly 8–10 Hz lower than experiment, all of the key trends for both rotamers

are reproduced. The close accord between theory and experiment across such a broad range of observables gives us confidence that the computed electron densities, along with the Kohn–Sham and NBOs, provide a firm foundation for exploring the origins of the α- and β-agostic distortions in these early-transition-metal systems.

In both α- and β-agostic isomers, the region between the metal center and the C−H bond is characterized by low and rather uniform electron density. The fact that *only* functionals that adhere to the UEG limit can reproduce the β-agostic geometry shows that an accurate description of this near-homogeneous region is critical, which, in turn, suggests that direct through-space interactions between the C−H bond and niobium *do* contribute to the stabilization of the structure. The location of Nb···H BCPs is consistent with this proposal, although the uniformity of the electron density profile in this region makes the molecular graph extremely sensitive to functional even though the optimized geometry is not. The α-agostic rotamer has very different characteristics: the structural parameters are very similar for UEG and non-UEG functionals, implying that an accurate description of the uniform electron density in the Nb···H region is *not* essential in this case. Consistent with this, no evidence of a Nb···H critical point has been found for any functional in the case of **1**. On this basis, we conclude that a direct interaction between the metal and C−H bond is not the driving force for the α-agostic distortion.

The Kohn–Sham and NBOs of the two rotamers suggest an alternative stabilizing mechanism for the α-agostic distortions that is, in fact, common to both α and β isomers. Delocalization of the electrons in the Nb−C_α bond into a π^* orbital of the alkyne ligand causes the Nb−C_α σ bonding orbital to tilt off the Nb−C axis, and this canting at the α carbon naturally forces one of the three substituents on C_α into an agostic position. In addition to this delocalization of the Nb−C_α bonding orbital that is common to both types of agostic distortion, the β-agostic isomer is further stabilized by a direct through-space interaction between the C−H σ orbital and the metal center.

The identification of delocalization of the Nb−C_α bonding electrons as a common driving force in both α- and β-agostic structures strikes resonance with the arguments of both Scherer[15] and Eisenstein.[8] The underlying cause is the relatively poor energy match between the lone pair on the formally anionic alkyl ligand and the high-lying d orbitals of an early transition metal, which forces the system to seek alternative sinks for the electron density in the Nb−C_α bond. This sink can be (i) vacant orbitals on the alkyl substituent (negative hyperconjugation),[15] (ii) vacant d orbitals on the metal,[8] or (iii) vacant π^* orbitals on an unsaturated coligand such as an alkyne. In each case, the reorientation of the lone pair on the α carbon toward the acceptor orbital naturally displaces it off the M−C axis, pushing one of the substituents toward the metal and hence driving the α- or β-agostic distortion.

Computational Details

In a recent benchmark study,[18] we demonstrated the fundamental importance of the UEG correlation limit for the DFT treatment of the β-agostic isopropylniobium complex. The hybrid PBE0 functional[35,36] (also known as PBE1PBE) emerged as one of the best performers among all of the functionals evaluated, so it is used throughout the present study unless stated otherwise. Valence triple-ζ polarized basis sets by Ahlrichs (TZVP) were used for chloride and for the atoms of the isopropyl ligand.[37] Valence double-ζ polarized (SVP) basis sets were used for all atoms of the alkyne ligand and the Tp^{Me2} backbone, whereas unpolarized SV basis sets were used for Tp^{Me2} substituents.[38] The alkyne ligand was modeled as MeC≡CMe; test calculations have shown that the replacement of Ph by Me has a negligible influence on any of the important structural, energetic, or spectroscopic parameters. Niobium was described with the [6s5p3d] SDD valence basis set and the quasi-relativistic ECP28MWB effective core potential of Andrae et al.[39] Geometries were fully optimized without any restrictions, and transition states were located mainly through the use of the STQN algorithm.[40] Stationary points were confirmed to be either minima or first-order saddle points by analytical calculation of their harmonic vibrational frequencies. The potential energy surface shown in Figure 1 was obtained by interpolating between the six stationary points. All calculations were performed with the *Gaussian03* series of programs.[41] NBO analyses were performed with inclusion of the 3-center bond option in the search algorithm.[34] Electron densities were obtained by single-point calculations with the all-electron DGDZVP basis set for niobium, and the topological analysis and construction of density maps and molecular graphs were carried out with the *AIM2000* program.[42] Spin–spin coupling constants were computed using the GIAO formalism.[43]

Supporting Information Available: Complete ref 41 and optimized Cartesian coordinates and total energies for all stationary points reported in Figure 1 (Table S1). This material is available free of charge via the Internet at http://pubs.acs.org.

OM701211R

(35) Perdew, J. P.; Burke, K.; Ernzerhof, M. *Phys. Rev. Lett.* **1996**, *77*, 3865.
(36) Perdew, J. P.; Ernzerhof, M.; Burke, K. *J. Chem. Phys.* **1996**, *105*, 9982.
(37) Schäfer, A.; Huber, C.; Ahlrichs, R. *J. Chem. Phys.* **1994**, *100*, 5829.
(38) Schäfer, A.; Horn, H.; Ahlrichs, R. *J. Chem. Phys.* **1992**, *97*, 2571.
(39) Andrae, D.; Haeussermann, U.; Dolg, M.; Stoll, H.; Preuss, H. *Theor. Chim. Acta* **1990**, *77*, 123.
(40) Peng, C.; Ayala, P. Y.; Schlegel, H. B.; Frisch, M. J. *J. Comput. Chem.* **1996**, *17*, 49.
(41) Frisch, M. J., et al. *Gaussian 03*, revision D.02; Gaussian, Inc.: Wallingford, CT, 2004. The complete citation is given in the Supporting Information.
(42) Biegler-König, F.; Schönbohm, J. *AIM2000*, version 2.0; Büro für Innovative Software: 2002.
(43) Lee, A. M.; Handy, N. C.; Colwell, S. M. *J. Chem. Phys.* **1995**, *103*, 10095.